Resonant Electron Capture in Violent Proton-Hydrogen Atom Collisions*

GRANT J. LOCKWOOD AND EDGAR EVERHART
Physics Department, University of Connecticut, Storrs, Connecticut
(Received August 21, 1961)

A new collision chamber design has made possible differential measurements of scattering of protons on atomic hydrogen target atoms. The scattering takes place in the interior of a furnace where hydrogen gas is dissociated. Electron capture probability is measured vs proton energy for protons passing nearly through the center of isolated hydrogen atoms such that the incident particle is scattered through an angle of 3°. This shows a resonant structure with maxima at energies of 0.78, 1.57, 3.92, and 20.1 kev. A simple model is presented for looking at these resonances. In the light of this model and previous theoretical work, the location of the high-energy maximum is unexpectedly low, and this suggests that a phase constant is needed to achieve agreement between experiment and theory. The H^+ on H data presented here are compared with those for the other combinations, H^+ on H_2, H^+ on He, and He^+ on He, which also show resonant electron capture.

1. INTRODUCTION

RESONANT electron capture in violent collisions was first detected by Ziemba and Everhart,[1] who studied the combination He^+ on He. The phenomenon was subsequently studied in several other ion-atom combinations, notably H^+ on He, and H^+ on H_2, by Ziemba *et al.*[2] Inasmuch as the greatest theoretical interest centers around the simplest ion-atom combination, protons incident on atomic hydrogen target atoms, an apparatus was especially designed for this experiment.

There have been total cross-section measurements by Fite *et al.*[3] of electron capture in the collisions of protons with atomic hydrogen, but their measurements are concerned with quite a different phenomenon. The total cross-section is an average over all impact parameters, and gentle collisions (those with large impact parameters) predominate.

The present paper, however, is concerned with differential measurements and studies only those particles which have been scattered to an appreciable angle (arbitrarily set at 3°, laboratory coordinates). This restricts the attention to those rare violent collisions wherein the incident proton passes practically through the center of the target hydrogen atom. When the electron capture probability is plotted vs the proton energy, four sharp peaks are found. An explanation is that the electron is oscillating between two energy levels where the number of oscillations depends on the duration of the collision.

Section 2 below describes the apparatus with particular attention to the target chamber and tests for atomic hydrogen. Section 3 shows the data for H^+ on H and also compares these with the H^+ on H_2 data. Section 4 discusses the data. A simple calculation is made of the spacing of the peaks which agrees approximately with the experimental values. A phase constant is introduced, not predicted theoretically, but required by the experimental data.

Ziemba and Russek[4] have given a theoretical treatment of resonant electron capture in the He^+ on He case. Our interpretation of the present H^+ on H case follows the plan of their treatment in some ways but is a simplified and possibly more general approach.

2. THE EXPERIMENT

Previous scattering experiments[3,5] with atomic hydrogen have used a difficult and ingeneous technique wherein an atomic beam is crossed with a beam of protons or electrons. This method is here quite impractical because the density of atomic scattering centers produced in an atomic beam is far too low for the present experiment. The differential cross sections which are measured here are very many times smaller that the total cross sections measured previously. Our apparatus is therefore constructed so that the scattering takes place *within* a furnace where the density of scattering centers can be made sufficiently large and where the temperature is high enough so that the hydrogen gas is almost entirely atomic. This new arrangement makes feasible differential measurements of single collisions on atomic hydrogen atoms.

(a) Apparatus and Procedure

The University of Connecticut 200-kv heavy-ion accelerator was used in this work. Much of the interesting data were to be found at energies below a few kev, and previously the ion beam had been rather unstable at these low energies. The difficulty was believed to be caused by erratic charges on thin oxide layers on metal surfaces. Therefore, all metal surfaces adjacent to the ion beam were coated with colloidal graphite or were gold plated. This modification made the proton beam stable even to energies as low as 0.7 kev and greatly reduced the scatter of the data points. (It was noted, however, that surfaces coated with colloidal graphite tend to cause a gaseous discharge of some sort even at

* This work was sponsored by the U. S. Army Research Office, Durham.
[1] F. P. Ziemba and E. Everhart, Phys. Rev. Letters **2**, 299 (1959).
[2] F. P. Ziemba, G. J. Lockwood, G. H. Morgan, and E. Everhart, Phys. Rev. **118**, 1552 (1960).
[3] W. L. Fite, R. T. Brackmann, and W. R. Snow, Phys. Rev. **112**, 1161 (1958); W. L. Fite, R. F. Stebbings, D. G. Hummer, and R. T. Brackman, Phys. Rev. **119**, 663 (1960).
[4] F. P. Ziemba and A. Russek, Phys. Rev. **115**, 922 (1959).
[5] W. L. Fite and R. T. Brackmann, Phys. Rev. **112**, 1141 (1958).

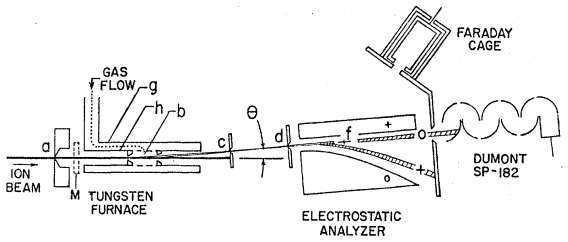

FIG. 1. The collision chamber and the associated detection apparatus.

fairly high vacuum conditions if they are in a region of high electric field. This phenomenon is not completely understood, but we would recommend gold plating in high field regions.)

Figure 1 shows the collision chamber (which is a tungsten furnace), the defining slits, the electrostatic analyzer, and the detecting system. A detailed description of the furnace is given in part **b** below. The incident proton beam passing through the furnace encounters atomic hydrogen target gas in the vicinity of *b*, and a very few of these protons individually undergo a single violent collision with a hydrogen atom such that they are scattered to an appreciable angle. (If the collision is not a violent close encounter, the scattering angle is negligibly small.) Holes *c* and *d*, preceding the electrostatic analyzer, select some of these particles which have been scattered to the particular angle θ of 3°. During the course of the violent collision the incident proton may or may not have captured the electron from the target hydrogen atom, and, thus, the particles passing through the electrostatic analyzer consist of a mixture of hydrogen atoms and protons. When both the curved and flat analyzer plates are grounded, all these particles reach the first dynode of a secondary electron multiplier and are counted. However, when a sufficient positive potential is applied to the flat analyzer plate the protons are swept out, and the hydrogen atom component is alone counted. The properties of the detecting system and the counting procedures are fully discussed in the paper by Ziemba *et al.*[2]

When the counting rate for neutral particles is divided by the counting rate for combined neutral and charged particles, a quantity P_0 is determined. This quantity is the fraction of scattered particles which are neutral and is also the probability that the incident proton has captured an electron in a single violent collision with a hydrogen atom. On a typical determination of P_0 at a chosen energy, there were several thousand scattered particles analyzed and counted. After each run the hydrogen target gas supply was turned off and the run repeated with residual gas. The correction for scattering from residual gas was always small, ranging from 1% to 10%.

(b) The Atomic Hydrogen Furnace

The experiments of Langmuir[6] and of Fite and Brackmann,[5] as well as calculations by Woolley, Scott, and Brickwedde[7] and by Bredt,[8] have all shown that hydrogen gas is practically entirely atomic at 2400°K provided that the hydrogen pressure is sufficiently low—of the order of 10 microns or less. There is good evidence[5,6] that the thermal accomodation coefficient is high for hydrogen on tungsten, and that only a few collisions on hot tungsten walls suffice to ensure equilibrium of the hydrogen.

The furnace illustrated schematically in Fig. 1 was designed to fulfill the above conditions. The outer tungsten tube *g* is 12.7 mm in diameter and 50.8 mm long. It is rolled from a 50.8-mm×76.2-mm sheet of 0.025-mm tungsten. At the ends it is supported in molybdenum sleeves which are pressed into massive water-cooled copper supports. These supports bring in the heating current (typically 325 amperes dc at 2.75 volts) in a radially symmetrical manner so that there is no magnetic field along the ion beam path. There is triple radiation shielding which is coaxial with outer tube *g* and this shielding has line-of-sight holes so that an optical pyrometer can be used to measure the temperature of the midpoint of *g*. There is an inner furnace tube *h*, which is 6.35 mm in diameter and 58.4 mm long, rolled from a 58.4-mm×40.6-mm sheet of 0.025-mm tungsten. It is supported on molybdenum sleeves and copper as was tube *g*, and it also carries current. There are two tungsten buttons 12.7 mm apart equally spaced on either side of *b* which are rolled into *h*. These buttons are each 3.2 mm thick and have 1.27-mm central holes with tapered edges as shown. This inner element *h* is preheated in a vacuum before final assembly to embrittle it, and then its wall is perforated between the buttons. The space between tubes *g* and *h* is packed with tungsten wool made from 0.025-mm tungsten wire.

The hydrogen gas, at a pressure of about two microns (cold), enters the region between *g* and *h* and flows through the tungsten wool. The purpose of this wool is two-fold; it ensures that many collisions will occur to help the hydrogen reach thermal equilibrium before reaching the inner furnace, and it acts as a multiple radiation shield so that the inner furnace may be kept at high temperature with a minimum of power. The hot hydrogen then passes through the perforations in *h* and reaches the scattering chamber. Each atom makes about 100 collisions in this hot region before leaving through the holes in the tungsten buttons, and in this region is practically entirely atomic as will be shown below. The gas escaping through the holes in the buttons is pumped away rapidly, so that there is a low concentration of atoms along the proton beam path except in the scattering region. There are heat shields to protect the copper buttons containing defining holes *a* and *c*.

Just to the right of hole *a* there is a movable monitor electrode *M*, which measures the ion beam before it enters the furnace. There is a collimating hole (not shown) preceding hole *a*, and these two holes, each

[6] I. Langmuir, J. Am. Chem. Soc. **37**, 417 (1915).

[7] H. W. Woolley, R. B. Scott, and F. G. Brickwedde, Bur. Standards J. Research **41**, 379 (1948). See p. 393.

[8] I. Bredt, Z. Naturforschung **6a**, 103 (1951).

0.51 mm in diameter, insure that the ion beam passes through the center of the furnace. The holes in the tungsten buttons are large enough, so that neither the original ion beam nor the particles scattered through angle θ from the region of b touch these buttons. Holes c and d are 0.25 mm and 0.61 mm in diameter, respectively, and are located, in turn, 33.1 mm and 60.6 mm from the scattering center b.

(c) Test for Atomic Hydrogen

With this apparatus it was possible to make an indirect experimental test for atomic hydrogen. Data were taken measuring P_0 for 3° scattering with the furnace first at room temperature and then at successively higher temperatures. This experiment was performed several times, and large differences were found between the molecular hydrogen and the presumed atomic hydrogen scattering cases. The data shown in Fig. 2 illustrate this test. The fraction P_0 of those scattered protons which have captured an electron is plotted vs the temperature of the inner furnace. The data are taken at 3.90 kev, which (as will be seen) is an energy for which there is a particularly marked difference between the molecular and atomic data. The curve of P_0 vs temperature in Fig. 2 is flat at 52% from room temperature to about 1500°K, and then it rises rapidly and again levels out at about 90% at 2400°K and above. All of the H^+ on H data to follow were taken at 2400°K, and the H^+ on H_2 comparison curve was run either at 1200°K or at room temperature. In taking the data for this curve, the mass rate of flow hydrogen through the furnace was held constant. At room temperature the pressure of the gas about to enter the furnace was two microns. The pressure within the furnace when cold was necessarily less than this. When the furnace was heated to 2400°K the density of the scattering centers dropped threefold, as measured from the number of particles scattered to 3° with constant incident proton beam.

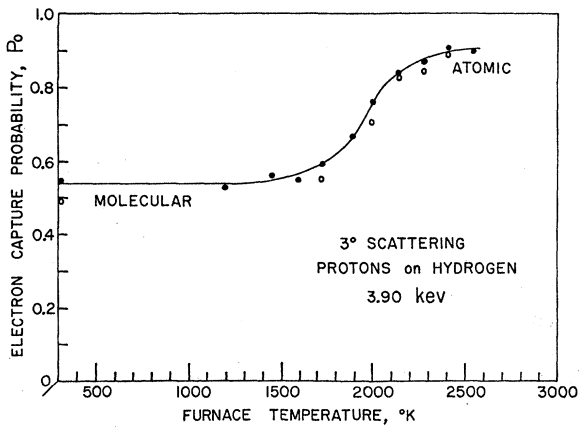

FIG. 2. The value of electron capture probability P_0 is plotted vs the inner furnace temperature for 3° scattering of H^+ on hydrogen at 3.90 kev. At low temperatures the gas within the furnace is molecular hydrogen, and at high temperatures it is atomic hydrogen. The hollow points and the solid points represent two separate data runs taken, respectively, at the beginning and at the end of the entire experiment.

The inner furnace temperature could not be measured directly because the inner region is completely enclosed, and there was no line-of-sight available to an optical pyrometer when scattering data were being taken. However, a preliminary calibration of the furnace assembly was made with some of the particle detecting apparatus removed so that an optical pyrometer could then be used to measure the temperatures of the inner and outer furnace elements in turn. This established a calibration of the relation between inner furnace temperature and outer furnace temperature. Later, in obtaining the temperatures for Fig. 2, the outer furnace temperature was measured, and the above calibration was used to find the corresponding inner furnace temperature. The temperature conditions of the inner element are those for which others[5] have found hydrogen to be almost entirely dissociated, and we regard Fig. 2 as showing the presence of substantially complete dissociation of hydrogen in the furnace.

(d) Choice of Scattering Angle

The 3° value of scattering angle θ was chosen as the largest feasible angle for these measurements. Of course, if this angle were made larger, the particles detected would arise from more violent collisions in the sense that the incident protons would pass even closer to the center of the target atom. However, the number of scattered particles drops precipitously with increase in θ making measurements difficult and inaccurate. The 3° angle of the present experiment is considered representative of violent collisions except at the lowest energies studied. The low-energy data are slightly affected by an increase in impact parameter and this is discussed in Sec. 4c below.

The values of P_0 do not depend on scattering angle, provided that this angle is large enough and the energy is not too low. The criterion is that the impact parameter be small compared to significant atomic dimensions, and this is largely fulfilled in the present experiment. This was confirmed experimentally for other light ion-atom combinations, H^+ on He and He^+ on He, in angular data runs (unpublished), and the 3° data for H^+ on H_2 presented in Sec. 3 below are substantially the same as those taken previously[2] at 5°.

3. DATA

The data for electron capture in violent collisions of H^+ on H are shown in Fig. 3. The electron capture probability P_0 is very high at incident proton energies of 20.1, 3.92, 1.57, and 0.78 kev and very low at 7.69, 2.39, and 1.11 kev. The data for the case H^+ on H_2 are also shown. This molecular case was measured earlier as seen in Fig. 4(b) of reference 2, but the present data is more accurate because the proton beam in the accelerator is now stable at low energies. The molecular data shows peaks which are much less pronounced than those in the atomic case although they are nearly in the same

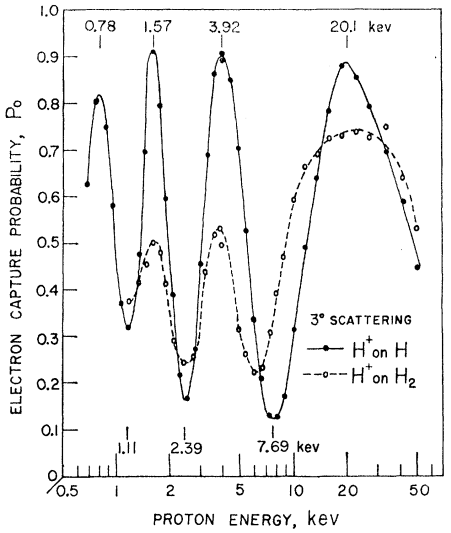

FIG. 3. The electron capture probability P_0 is plotted vs incident proton energy in kev for the combinations H^+ on H and H^+ on H_2. These data are for violent collisions in which the scattered particles emerge at 3°; laboratory coordinates.

locations. However, the valley at 6 kev in the H^+ on H_2 case is clearly shifted from the corresponding valley at 7.69 kev in the H^+ on H case.

The peaks in the atomic case reach about 90% at the highest and the valleys reach no lower than 12%. It was necessary to consider the possibility that the peaks and valleys should reach 100% and 0% respectively and that perhaps experimental difficulties prevented this result. To explore this possibility several tests were made:

(1) The machine was set on the peak at 3.92 kev and again on the valley at 7.69 kev, and the hydrogen pressure varied with the furnace hot. The value of P_0 did not depend on the rate of flow of hydrogen gas through the furnace even when this rate was doubled or tripled by increasing the pressure in the feed lines above the normal two microns. This test assures that the density of scattering centers was sufficiently low for single collision studies. It also shows that neither the incident beam nor the scattered particles were appreciably modified by passing through the residual gas outside the furnace.

(2) The temperature run of Fig. 2, taken at a peak of the curve, shows no indication that the probability P_0 would rise much above 91% at still higher temperatures. Certainly it would not rise to 100%. Thus the fraction of hydrogen dissociated is already arbitrarily high, and still higher dissociation would not raise the curve to 100%.

(3) The energy resolution on our machine is 0.1% and is not responsible for any broadening of the peaks and valleys. The absolute voltages on the accelerator are also determined to 0.1%.

Our conclusion is that there are no significant errors and that the H^+ on H data is given correctly as in Fig. 3 within the scatter of the data points.

4. DISCUSSION AND THEORY

When the H^+ on H data are plotted vs reciprocal velocity as in Fig. 4, it is seen that the maxima and minima are nearly equally spaced. This experimental fact has been noted for the several other combinations which show resonant electron capture.[1,2]

(a) The Spacings of the Resonances

The discussion which follows presents a simple model for looking at these resonances. It is related to certain aspects of a theoretical formulation by Bates, Massey, and Stewart.[9] In conjunction with the experimental data, it is hoped that our model will shed new light on the theoretical approaches to the problem.

One way to calculate the spacing between the peaks of Fig. 4 is to find the difference between the "time of transit" of the ion for two consecutive peaks. Suppose that t_1, t_3, t_5, t_7 are the times characteristic of the several peaks in turn, and that t_2, t_4, t_6 are the times for the valleys. Then, for example, t_3-t_1 is the difference in time of transit for two events which both resulted in high values of P_0, and the assumption is made that t_3-t_1 is the period T_1 for one cycle of electronic oscillation.

These times t_n are related to the corresponding velocities v_n by $t_n=a/v_n$, where a is the distance over which the collision occurs. Then

$$T_1=t_3-t_1=(a/v_3)-(a/v_1)=h/E. \tag{1}$$

Here it is further assumed that the period may be set equal to Planck's constant h divided by an interaction energy E associated with the oscillation. Equation (1) is generalized and written as

$$\langle Ea\rangle_n=\frac{h}{(1/v_{n+2})-(1/v_n)}, \tag{2}$$

in which the right side contains the measured velocities corresponding to adjacent peaks (valleys). The significant experimental fact is that values of $\langle Ea\rangle_n$ calculated from this equation are largely independent of n. Neither E nor a on the left side are precise concepts and the angular brackets are drawn to indicate an "effective value" of this quantity which is, dimensionally, energy times length. Certainly the collision begins and ends gradually so that a fixed a is an oversimplification, and also the interaction energy E will vary with internuclear separation. It is suggested that the effective

[9] D. R. Bates, H. S. W. Massey, and A. L. Stewart, Proc. Roy. Soc. (London) **A216**, 437 (1953), see Eq. (134).

value of $\langle Ea\rangle$ might be calculated using

$$\langle Ea\rangle=\int_{-\infty}^{+\infty}E(s)ds, \tag{3}$$

where ds is an element of the path of the incident particle, and $E(s)$ is the interaction energy at s along the path. Although the above development is certainly not rigorous, Eq. (3) is reasonable, and very interesting results follow when it is compared with the experimental values of $\langle Ea\rangle$ obtained through Eq. (2).

An integral equivalent to that of Eq. (3) appears in the other formulation[4,10] of this problem, and $E(s)$ is taken as the energy difference between the first symmetric wave function and first antisymmetric wave function of the system.

For the H^+ on H case the collision is regarded as

$$H^++H\rightarrow(H_2^+)\rightarrow(He^+)\rightarrow(H_2^+)\rightarrow H+H^+. \tag{4}$$

Thus, as the proton approaches the hydrogen atom the wave functions are presumed to be adiabatically those of the H_2^+ ion with varying internuclear separation R. At essentially zero separation the wave functions (if not the nucleus) are those of the He^+ ion. The process reverses during the second half of the collision. Bates, Ledsham, and Stewart[11] have calculated the wave functions and their energies for the H_2^+ ion. Using their notation for the energy states in question,

$$E(s)=E(1s\sigma_g)-E(2p\sigma_u). \tag{5}$$

This energy difference is shown vs R in Fig. 5(a) and is taken for the integrand in Eq. (3).

The integration path for Eq. (3) is illustrated in Fig. 5(b) which shows the classical path (dotted) of the incident proton colliding with a hydrogen atom. The scattering angle θ is only a few degrees here, and the dotted path will be replaced in the integration by the straight path s, which lies at the same distance r_0 of closest approach. Here r_0 is only slightly greater than the impact parameter.

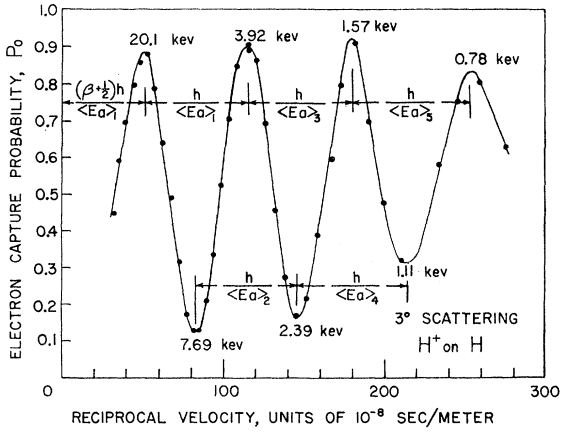

FIG. 4. The electron capture probability P_0 for violent collisions of H^+ on H is plotted vs the reciprocal of the incident proton velocity. The even spacings, identified by the several $h/\langle Ea\rangle$ labelings, are characteristic of resonant electron capture.

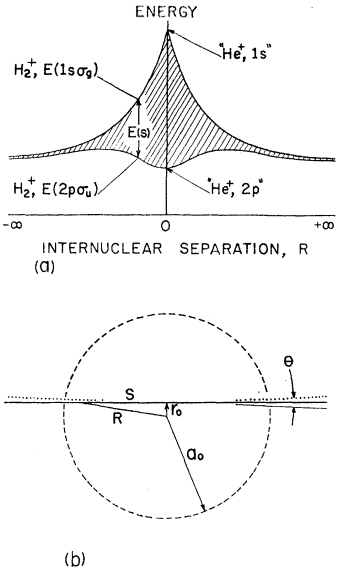

FIG. 5. (a) The energies of the first symmetric and the first antisymmetric electronic wave functions of H_2^+ are plotted vs internuclear separation R. For $R=0$ the wave functions reduce to those of the He^+ ion. (b) The path of a proton making a violent collision with a hydrogen atom (of approximate size a_0) is shown dotted. For calculations where the scattering angle θ is small, this dotted path is replaced by the straight line s which misses the target nucleus by the same distance r_0 of closest approach.

An integration equivalent to Eq. (3) was carried out by Ziemba[10] for the H^+ on H case, following the pattern of the Ziemba-Russek[4] paper. He predicted, nearly correctly, the spacings of the resonant peaks, but did not note the phase constant β (to be discussed below), and so did not predict their location in energy correctly. For the high energy peaks, r_0 is approximately zero and his evaluation, equivalent to Eq. (3), using Eq. (5), yields $\langle Ea\rangle=9.76$ rydberg—a_0 units, or 70.2 ev-A.

Our experimental value of $\langle Ea\rangle$, determined using Eq. (2) from the velocities corresponding to the first and second maxima of Fig. 4, is 63.7 ± 1 ev-A. The calculated value agrees fairly well with the experimental value, but it is well outside the limits of experimental error.

(b) The Phase Constant β

An empirical equation which correctly reproduces the experimental data of Fig. 4 is

$$P_0=K_1(1/v)+K_2(1/v)\sin^2[(\pi\langle Ea\rangle/vh)-\beta], \tag{6}$$

where K_1 and K_2 are slowly varying functions of reciprocal velocity. If $K_1=0$, $K_2=1$, and $\beta=0$, the equation is in the same form as that derived by Bates, Massey, and Stewart,[9] and used by Ziemba and Russek[4] in discussing He^+ on He. From Fig. 4 it is evident that K_1 is greater than zero and K_2 is less than unity.

The phase constant β has the experimental value of $(0.28\pm0.01)\pi$. This was unexpected on the basis of the simple model presented here. It would have been

[10] F. P. Ziemba, Doctoral thesis, University of Connecticut, 1960 (unpublished), p. 36.
[11] D. R. Bates, K. Ledsham, and A. L. Stewart, Phil. Trans. Roy. Soc. A246, 215 (1953).

TABLE I. The experimental values of $\langle Ea \rangle$ in electron volt Angstroms (for very small values of r_0) and the values of the phase constant β are given for three ion-atom collision combinations.

Combination	$\langle Ea \rangle$ (ev-A)	β
H^+ on H	63.7±1	$(0.28\pm0.01)\pi$
H^+ on He	84.6±1	$(0.26\pm0.02)\pi$
He^+ on He	102±3	$(0.23\pm0.08)\pi$

supposed that the proton whose velocity corresponded to the highest energy peak in P_0 had sufficient time during the collision for just half an oscillation cycle, and this would correspond to $\beta=0$. The experimental value of $\beta=0.28$ corresponds to 0.78 of a cycle for this first transition.

It is not clear to the present authors that Eq. (134) of reference 9, which was the basis for all previous work[4,10] should be critized for its omission of K_1, K_2, and β which appear in Eq. (6). It is quite likely that the present experiment does not entirely duplicate the conditions required for the validity of their Eq. (134) and that Bates, Massey, and Stewart did not envisage its exact application to the present situation.[12]

Three ion-atom combinations showing pronounced resonant electron capture effects have been studied to date, and Table I summarizes the experimental results. The values of $\langle Ea \rangle$ and β for the He^+ on He and for the H^+ on He cases were obtained by a re-analysis of the original data used for Fig. 4(a) and 4(c) of reference 2.

(c) Behavior at Low Energies

At low energies, moving to the right in Fig. 4, the spacings of the peaks becomes progressively wider, and this corresponds to a decrease in $\langle Ea \rangle$. The experimental values of $\langle Ea \rangle$, obtained using Eq. (2) with the velocities corresponding to successive peaks (valleys), are listed in Table II, where each $\langle Ea \rangle$ value is identified according to its subscript n in Fig. 4.

The observed decrease in $\langle Ea \rangle$ at low energies may be predicted theoretically. When the scattering angle is held fixed, the distance r_0 in Fig. 5(b) increases at low energies. Each peak (valley) has its own r_0 value, and this is readily estimated using classical orbits with allowance for electron screening.[13,14] The average value of r_0 is tabulated for each pair of peaks (valleys) in question. Using $E(s)$ from Eq. (5), the integral of Eq. (3) was evaluated numerically for each corresponding

TABLE II. A comparison of the experimental and calculated values of $\langle Ea \rangle$ for the successive peaks of Fig. 4.

Spacing Identification Subscript n	Experimental $\langle Ea \rangle$ (ev-A)	Calculated $\langle Ea \rangle$ (ev-A)	Average r_0 (A)
1	63.7	70.0	0.041
2	63.6	69.6	0.073
3	61.8	68.9	0.114
4	60.0	67.8	0.162
5	54.5	66.0	0.219

average r_0 value, and these calculated values of $\langle Ea \rangle$ are shown in Table II for comparison with the experimental values. There is qualitative agreement for the decrease in $\langle Ea \rangle$. However, the calculated values exceed the experimental values by 6 to 8 ev-A in most cases.

(d) He^+ on He and H^+ on He

There may be some difficulties in applying the present simple treatment to other combinations. For example, in the He^+ on He case, as the two atoms approach closely, the system should have the electronic wave functions of Be^+, whose ionization potential is only 18 ev. The difference between any symmetric and any antisymmetric wave functions for the outer electron cannot be larger than this. It would therefore seem impossible, using a reasonable interaction length, for an integral as in Eq. (3) to attain a value of 102 ev-A which is the experimental result. The Ziemba-Russek paper[4] treating this problem did achieve reasonable agreement with experiment, but did not justify their assumed value of $E(s)$ which reached 107 ev at $R=0$. However, the total electronic energy of Be^+ is 388 ev and those of the separated particles, He^+ and He, total 133 ev, leaving a change of energy of 255 ev during the collision. Thus, if the energies and oscillations of all three electrons contribute to the effect, there is sufficient interaction energy over a reasonable path length to agree with the experimental value of 102 ev-A given in Table I.

The H^+ on He case is more hopeful. At nearly rezo separation the system should have the wave functions of Li^+, which has an ionization potential of 75 ev. In this case it is possible for $E(s)$ to reach nearly this magnitude. With a reasonable interaction length it is quite possible that the integral of Eq. (3) could be near 85 ev-A which is the experimental value for this combination.

ACKNOWLEDGMENTS

We are grateful to Dr. Francis P. Ziemba and Professor Arnold Russek for discussions of the theory and to Professor D. R. Bates for helpful correspondence. We thank Mr. Gerry H. Morgan and Mr. Herbert F. Helbig who helped to operate the accelerator.

[12] *Note added in proof.* A paper by D. R. Bates and R. McCarroll [Proc. Roy. Soc. (London) **A245**, 175 (1958)] has come to our attention. This improved general formulation of ion-atom collision theory has evident applications to the present experiment.

[13] E. Everhart, G. Stone, and R. J. Carbone, Phys. Rev. **99**, 1287 (1955).

[14] G. H. Lane and E. Everhart, Phys. Rev. **117**, 920 (1960). Equation (6) of this reference is used with the screening length arbitrarily at $a=0.53\times10^{-8}$ cm.